Ambiguities in the Scattering Tomography for Central Potentials

Awatif Hendi,[1,2] Julian Henn,[2] and Ulf Leonhardt[2]

[1]*Science and Medical Studies, Female Section, King Saud University, P.O. Box 22452, Riyadh 11495, Saudi Arabia*
[2]*School of Physics and Astronomy, University of St. Andrews, North Haugh, St. Andrews KY16 9SS, Scotland, United Kingdom*
(Received 26 May 2006; published 14 August 2006)

Invisibility devices exploit ambiguities in the inverse scattering problem of light in media. Scattering also serves as an important general tool to infer information about the structure of matter. We elucidate the nature of scattering ambiguities that arise in central potentials. We show that scattering is a tomographic projection: The integrated scattering angle is a projection of a scattering function onto the impact parameter. This function depends on the potential but may be multivalued, allowing for ambiguities where several potentials share the same scattering data. In addition, multivalued scattering angles also lead to ambiguities. We apply our theory to show that it is, in principle, possible to construct an invisibility device without infinite phase velocity of light.

An invisibility device [1–7] should guide light around an object as if nothing were there. It is conceivable that such devices can be made using modern metamaterials [2–5,7]. Passive optical devices use spatially varying refractive-index profiles for imaging. Within the validity range of geometrical optics, index profiles of isotropic dielectric media are mathematically equivalent to potentials for light rays [4,8]. Therefore, such an invisibility device corresponds to a potential that has the same scattering characteristic as empty space. While the inverse scattering problem for waves has unique solutions [9], the scattering of rays may be ambiguous; i.e., different potentials may lead to identical scattering data. Here we show how such ambiguities arise in the case of radially symmetric potentials. Our theory indicates that it is, in principle, possible to construct an invisibility device where the phase velocity of light does not approach infinity, in contrast to all previous proposals for macroscopic cloaking [2–5]. This could inspire ideas for developing invisibility devices without anomalous dispersion [2] that could operate in a relatively wide frequency window. In addition to applications in a potentially new area for metamaterials, our theory has wider implications for the field of scattering tomography.

The inversion of the classical scattering in central potentials is a classic textbook problem that has made it into the exercises in Landau and Lifshitz's *Mechanics* [10]. Since Rutherford's experiments, scattering has served as an important tool to investigate the structure of matter, with modern applications ranging from biomedical research to astrophysics. Techniques to infer the structure of matter from scattering are often called scattering tomography, although, strictly speaking, they are not directly related to traditional tomography [12] where the shape of a hidden object is reconstructed from projections. Here we show that the case of scattering in central potentials literally is a tomographic projection in disguise but with an interesting twist: The object to be reconstructed corresponds to the potential but may be represented by a multivalued function, allowing for ambiguities.

Figure 1 illustrates the situation typical for scattering in central potentials. An incident ray characterized by the impact parameter b and the energy E is deflected by the angle χ. We use polar coordinates with radius r and angle φ in the plane orthogonal to the angular-momentum vector. The scattering angle is determined as [11]

$$\chi = \pi - 2 \int_{r_0}^{\infty} \frac{(b/r)dr}{\sqrt{\rho^2 - b^2}}. \qquad (1)$$

Here r_0 denotes the radial turning point of the trajectory given by b and E, and ρ represents the potential as

$$\rho = r \sqrt{1 - \frac{U(r)}{E}}, \qquad \frac{U}{E} = 1 - \frac{\rho^2}{r^2}. \qquad (2)$$

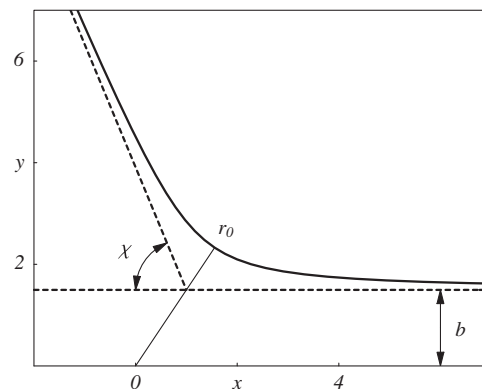The outermost turning point corresponds to the largest

FIG. 1. Scattering in a central potential. A trajectory incident with impact parameter b is deflected by the angle χ in the rotationally symmetric potential $U(r)$ centered at the origin, with $r = \sqrt{x^2 + y^2}$ in the Cartesian coordinates x and y. The turning point of the trajectory is denoted by r_0. The figure shows Rutherford scattering [11] in a repulsive $1/r$ potential.

value of r at which the denominator in the integrand (1) of the scattering angle vanishes, i.e., at which $\rho = b$. Reversing this relation leads to a physical interpretation for ρ: $\rho(r)$ describes the impact parameter for which the radius r is a turning point. Therefore, we may call ρ the turning parameter. Figure 2 illustrates the representation of the potential using the turning parameter. The largest zero of $\rho(r)$ corresponds to the potential barrier where $U = E$. The potential is repulsive for $\rho < r$, zero for $\rho = r$, and attractive for $\rho > r$. Note that the inverse function $r(\rho)$ may be multivalued, as shown in Fig. 2(a). The additional values of $r(\rho)$ describe the turning points of additional bound trajectories for the same energy E and the angular momentum that corresponds to the impact parameter b. Scattering does not probe such bound states, although the trajectories of scattered rays may enter the same region for different impact parameters b. As we show, the possibility of such elusive bound trajectories indicates ambiguities in scattering.

In the following, we express the description of scattering in central potentials as a tomographic projection for the integrated scattering angle
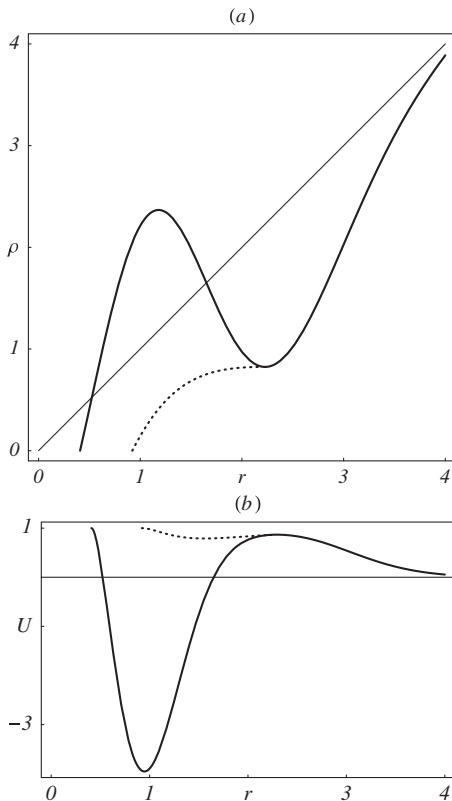
$$\phi = \int_{\infty}^{b} \chi \, db. \tag{3}$$

First, we represent Eq. (1) as

$$\chi = 2b\left(\int_{b}^{\infty} \frac{d\rho}{\rho\sqrt{\rho^2 - b^2}} - \int_{r_0}^{\infty} \frac{dr}{r\sqrt{\rho^2 - b^2}} \right)$$

$$= 2b \int_{b}^{\infty} \frac{W'}{a} \, d\rho \tag{4}$$

in terms of

$$W = \ln(\rho/r), \qquad a = \sqrt{\rho^2 - b^2}. \tag{5}$$

A prime indicates differentiation with respect to the turning parameter. We call W the scattering function. When $r(\rho)$ is multivalued, the integration contour is understood to follow accordingly. Since

$$\frac{d}{db} \int_{b}^{\infty} W' a \, d\rho + \int_{b}^{\infty} \frac{W' b}{a} \, d\rho = -W' a \big|_{\rho=b} = 0, \tag{6}$$

we obtain for the integrated scattering angle

$$\phi = -2 \int_{b}^{\infty} W' a \, d\rho = 2 \int_{b}^{\infty} W a' \, d\rho = \int_{-\infty}^{+\infty} W \, da. \tag{7}$$

This result has the simple geometrical meaning illustrated in Fig. 3: Imagine that a and b constitute a plane of impact parameters where one, b, is experimentally accessible and the other, a, is not. The scattering function W depends only on the radius $\rho = \sqrt{a^2 + b^2}$, both directly by definition (5) and in $r(\rho)$. Equation (7) shows that the integrated scattering angle is a projection of the rotationally symmetric object $W(\rho)$ onto the experimentally accessible impact parameter b in exactly the same way as objects are pro-
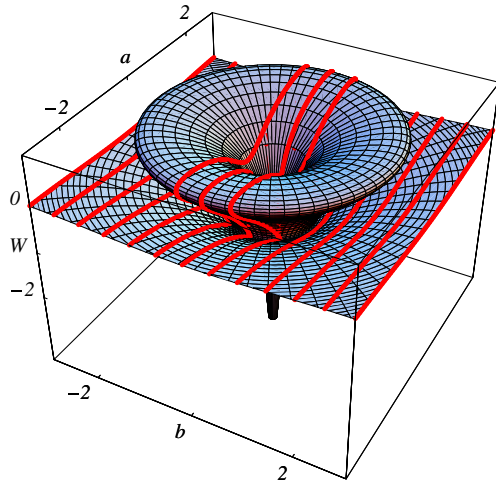

FIG. 2. Representation of the potential by the turning parameter ρ defined in Eq. (2). The solid line in (a) shows a fold in the turning parameter where $r(\rho)$ is multivalued. (b) shows the corresponding potential $U(r)$. The dotted lines describe $\rho(r)$ and $U(r)$ for a potential with the same scattering characteristics. Here $r(\rho)$ was obtained from Eq. (10) using the definition (5) of the scattering function W.

FIG. 3 (color online). Scattering tomography. The integrated scattering angle ϕ is a projection of the scattering function W onto the impact parameter b along the lines of the fictitious parameter a. The radius ρ in this auxiliary (a, b) plane is the turning parameter (2). The scattering function, defined in Eq. (5) and obtained from Fig. 2, may be multivalued, as shown here. The folds of W visualize the ambiguities of scattering.

jected in classical tomography [12] or Wigner functions in quantum tomography [13,14]. If $r(\rho)$ is single-valued, one can invert the projection by the inverse Abel transformation [13–15]

$$W = -\frac{1}{\pi}\int_\rho^\infty \frac{\chi db}{\sqrt{b^2 - \rho^2}}, \qquad (8)$$

a special case of the inverse Radon transformation [12,13]. If $r(\rho)$ is multivalued, one can hide features of the potential in the folds of W, as Fig. 3 illustrates.

Consider the scattering ambiguities where the scattering function W is multivalued. The simplest case corresponds to a single fold in W between two turning parameters ρ_1 and ρ_2, as shown in Figs. 3 and 4. We use the inverse Abel transformation (8) to construct a potential, described by $W_0(\rho)$, that exhibits the same scattering characteristics as W. Figure 3 indicates that W and W_0 agree for $\rho > \rho_1$, because all projections lie under the fold. For $\rho < \rho_1$, the scattering angle χ is, according to Eq. (1),

$$\chi = 2b\int_b^\infty \frac{W'd\sigma}{\sqrt{\sigma^2 - b^2}} + 2b\int_{\rho_1}^{\rho_2}\frac{W'_+ - W'_-}{\sqrt{\sigma^2 - b^2}}d\sigma, \qquad (9)$$

where the integration variable σ refers to the turning parameter, W follows the solid curve in Fig. 4, with a jump at ρ_1, whereas W_+ denote the top and W_- the bottom curve of the fold. Since the inverse Abel transformation (8) uniquely inverts the first term in χ, we obtain for the difference between W and W_0

$$W - W_0 = \frac{2}{\pi}\int_\rho^{\rho_1}\int_{\rho_1}^{\rho_2}\frac{b(W'_+ - W'_-)d\sigma db}{\sqrt{(b^2 - \rho^2)(\sigma^2 - b^2)}}$$

$$= \frac{2}{\pi}\int_{\rho_1}^{\rho_2}(W'_+ - W'_-)\arctan\left(\frac{\sqrt{\rho_1^2 - \rho^2}}{\sqrt{\sigma^2 - \rho_1^2}}\right)d\sigma$$

$$= \frac{2}{\pi}\int_{\rho_1}^{\rho_2}(W_+ - W_-)\frac{\sqrt{\rho_1^2 - \rho^2}}{\sqrt{\sigma^2 - \rho_1^2}}\frac{\sigma d\sigma}{\sigma^2 - \rho^2} \qquad (10)$$
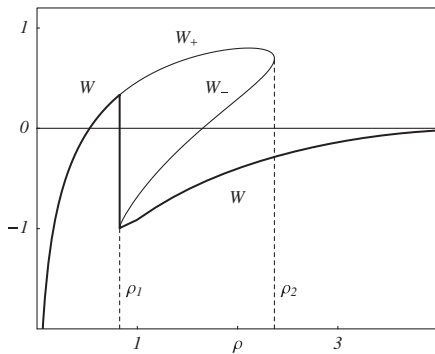

FIG. 4. Multivalued scattering function W obtained from Fig. 2 according to the definition (5). The $W(\rho)$ function is folded between the turning parameters ρ_1 and ρ_2 where W_+ denotes the top and W_- the bottom curve of the fold.

by partial integration, utilizing that the boundary term vanishes, because $W_-(\rho_2) = W_+(\rho_2)$. Since $W_+ > W_-$, the ambiguous W must exceed W_0 in the single-valued region inside ρ_1, which implies that the radius $r = \rho\exp(-W_0)$ is greater than $\rho\exp(-W)$. The fold of multivaluedness thus magnifies the scattering structure of the potential. In particular, for ambiguous scattering potentials, the zero of $\rho(r)$ is closer to the origin than for the equivalent nonambiguous one. Since this zero corresponds to the potential barrier beyond which one can hide, nothing is gained, quite the opposite. This feature continues in the general case of several folds in W, because one could replace W by equivalent single-valued W_0 with the same scattering characteristics, starting from the outmost fold and proceeding to the inside.

An alternative way of hiding the presence of a potential would be to let the trajectories leave at scattering angles that are multiples of 2π, i.e., to turn them around in precisely adjusted loops. Suppose that for impact parameters b smaller than a critical b_0 the trajectories are uniformly turned by $\chi = -2\pi\nu$ and are not affected for b larger than b_0. Here ν may be a real number, not only an integer, for the sake of generality. Assuming that $r(\rho)$ is single-valued, we obtain from the inverse Abel transformation (8)

$$r = \begin{cases} \rho(b_0/\rho + \sqrt{b_0^2/\rho^2 - 1})^{-2\nu} & \rho < b_0 \\ \rho & \rho \ge b_0. \end{cases} \qquad (11)$$

Figure 5 illustrates the curves of $\rho(r)$. Clearly, $r(\rho)$ is single-valued by definition. For $\nu < 0$, the potential would be repulsive, because the trajectories are deflected, but in this case the function $\rho(r)$ itself is multivalued. Consequently, no central potential exists that uniformly deflects trajectories. For $\nu > 0$, the potential is attractive, as one would expect to be necessary for bending trajectories around the center of force. The case $\nu = 1/2$ corresponds to a Kepler potential [11] or the Eaton lens [15–17] developed in radar technology. In the limit $\rho \to 0$, we get from Eq. (11) the asymptotics $\rho/r \sim (2/r)^{2\nu/(2\nu+1)}$, and, hence, according to Eq. (2) the potential U diverges with the power $-4\nu/(2\nu + 1)$ for small r. One cannot hide anything here. In the limit $\nu \to \infty$ of infinitely many cycles, U approaches near the origin the $1/r^2$ potential of fatal attraction [11]. Figure 5(b) illustrates the case where the trajectories are turned around by 2π.

Although one cannot directly apply the ambiguous scattering of isotropic and centrally symmetric media to construct an invisibility device, one can use their singularities to improve anisotropic devices. Such a device is designed to facilitate a coordinate transformation with a hole where anything inside is hidden by construction [2]. Consider a two-dimensional case in polar coordinates. Suppose that the radius r is mapped onto r' such that r' reaches the radius of the hole at $r = 0$ as
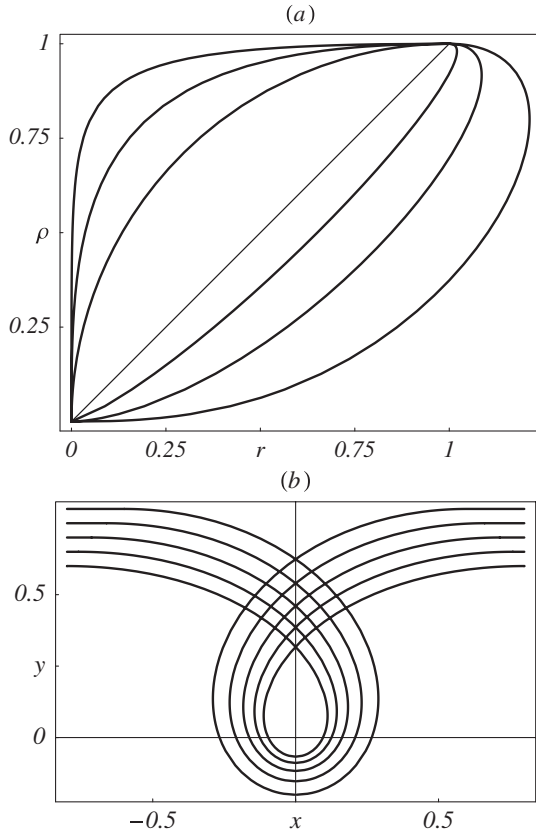
FIG. 5. Uniform bending. (a) shows the turning parameters obtained from Eq. (11) for the winding numbers $\nu \in \{2, 1, 0.5, -0.1, -0.2, -0.3\}$ and $b_0 = 1$. For negative ν, $\rho(r)$ is multivalued and, hence, unphysical. (b) illustrates the uniform loops of trajectories for $\nu = 1$.

$$\frac{\partial r'}{\partial r} \sim \alpha r^{-s} \quad \text{for} \quad r \sim 0, \tag{12}$$

where α and s are non-negative constants. Beyond the outer radius b_0 of the cloak, the coordinates r' shall coincide with r. Assume in unprimed space the isotropic and radially symmetric refractive-index profile $n(r)$ with perfect impedance matching. References [2,5] give recipes to calculate the dielectric ε and magnetic μ that facilitates the coordinate transformation (12). We find

$$\varepsilon'_r = \mu'_r \sim \frac{\alpha r^{1-s}}{r'} n(r), \qquad \varepsilon'_\varphi = \mu'_\varphi \sim r' \frac{r^{s-1}}{\alpha} n(r). \tag{13}$$

Suppose that we use a profile where $n^2/2$ corresponds [4] to the $E - U$ of uniform bending (11) with the definition (2) and $\nu = 1$. If we choose $s = 1/3$, the singularity of U compensates for the zero in the refractive index in real space that would otherwise imply [2] that the speed of light tends to infinity at the inner lining of the cloak. The phase velocity in radial direction is finite. On the other hand, the

speed of light in the angular direction tends to zero with the power 4/3. Our simple example indicates that invisibility devices with finite phase velocity are possible, in principle. In our case, wrapping light around the invisibility device stratifies the optical wavefronts. However, there is a price to pay: Light propagation with finite phase velocity around an object inevitably causes time delays that result in wavefront dislocations at the boundary [4]. The invisibility is perfect for rays but not for waves.

Conclusions.—We visualized the scattering of particles in central potentials. Scattering appears as a tomographic projection with an interesting twist: multivalued images that encode the potential. Multiple branches describe scattering ambiguities where different potentials lead to identical scattering data. Such ambiguities are limited, though: Central potentials are never completely invisible, but they can be employed to improve invisibility devices. Our theory proves that invisibility requires asymmetric refractive-index profiles [3,4] or anisotropic media [2,5]. Otherwise, trying to hide things uniformly from all sides just magnifies them.

[1] G. Gbur, Prog. Opt. **45**, 273 (2003).
[2] J. B. Pendry, D. Schurig, and D. R. Smith, Science **312**, 1780 (2006).
[3] U. Leonhardt, Science **312**, 1777 (2006).
[4] U. Leonhardt, New J. Phys. **8**, 118 (2006).
[5] U. Leonhardt and T. G. Philbin, cond-mat/0607418.
[6] M. Kerker, J. Opt. Soc. Am. **65**, 376 (1975).
[7] A. Alu and N. Engheta, Phys. Rev. E **72**, 016623 (2005); G. W. Milton and N.-A. P. Nicorovici, Proc. R. Soc. A (in press).
[8] M. Born and E. Wolf, *Principles of Optics* (Cambridge University Press, Cambridge, England, 1999).
[9] A. I. Nachman, Ann. Math. **128**, 531 (1988).
[10] Problem 7 in Sec. 18 of Ref. [11].
[11] L. D. Landau and E. M. Lifshitz, *Mechanics* (Pergamon, Oxford, 1976).
[12] G. T. Herman, *Image Reconstruction from Projections: The Fundamentals of Computerized Tomography* (Academic, New York, 1980); F. Natterer, *The Mathematics of Computerized Tomography* (Wiley, Chichester, 1986).
[13] U. Leonhardt, *Measuring the Quantum State of Light* (Cambridge University Press, Cambridge, England, 1997).
[14] U. Leonhardt and I. Jex, Phys. Rev. A **49**, R1555 (1994).
[15] J. H. Hannay and T. M. Haeusser, J. Mod. Opt. **40**, 1437 (1993).
[16] J. E. Eaton, Trans. IRE Ant. Prop. **4**, 66 (1952).
[17] M. Kerker, *The Scattering of Light* (Academic, New York, 1969).